HOKKAIDO UNIVERSITY

Title	Secondary bow with ripples in 12C+12C rainbow scattering
Author(s)	Ohkubo, Shigeo; Hirabayashi, Yoshiharu
Citation	European physical journal A : Hadrons and nuclei, 61(9) https://doi.org/10.1140/epja/s10050-025-01685-4
Issue Date	2025-09-16
Doc URL	https://hdl.handle.net/2115/98106
Rights	This version of the article has been accepted for publication, after peer review (when applicable) and is subject to Springer Nature's AM terms of use, but is not the Version of Record and does not reflect post-acceptance improvements, or any corrections. The Version of Record is available online at: https://doi.org/10.1140/epja/s10050-025-01685-4
Type	journal article
File Information	EPJA=12C+12Cbow-v11-1.pdf

Hokkaido University Collection of Scholarly and Academic Papers : HUSCAP

Secondary bow with ripples in ^{12}C+^{12}C rainbow scattering

S. Ohkubo[1*] and Y. Hirabayashi[2]

[1*]Research Center for Nuclear Physics, Osaka University, Ibaraki, 567-0047, Japan.
[2]Information Initiative Center, Hokkaido University, Hokkaido University, Sapporo, 060-0811 , Japan.

*Corresponding author(s). E-mail(s): ohkubo@rcnp.osaka-u.ac.jp;

Abstract

We report, for the first time, the emergence of a secondary bow with ripples in $^{\mathbf{12}}$C+$^{\mathbf{12}}$C nuclear rainbow scattering. This finding was achieved by studying the experimental angular distributions in $^{\mathbf{12}}$C+$^{\mathbf{12}}$C scattering at incident energies $\boldsymbol{E_L}$= 240 and 300 MeV, utilizing an extended double-folding model. This model accurately describes all diagonal and off-diagonal coupling potentials derived from the microscopic wave functions for $^{\mathbf{12}}$C. Although the observed angular distributions of rainbow scattering at large angles (approaching $\mathbf{90^\circ}$) are complicated by the symmetrization of two identical bosonic nuclei, the Airy minimum, associated with a dynamically generated secondary bow with ripples, is clearly identified at approximately 77° for 240 MeV in the fall-off region of the primary nuclear rainbow. This finding, along with previous findings in the $^{\mathbf{16}}$O+$^{\mathbf{12}}$C and $^{\mathbf{13}}$C+$^{\mathbf{12}}$C systems, reinforces the concept of a secondary bow in nuclear rainbow scattering.

Keywords: $^{\mathbf{12}}$C+ $^{\mathbf{12}}$C, nuclear rainbow, refractive scattering, secondary bow, ripples, double folding model, coupled channel method

1 Introduction

Rainbows have attracted humankind since long before the birth of science, and their mystery has been scientifically revealed since Descartes' time [1–5]. A microscopic nuclear rainbow discovered by Goldberg *et al* [6] is a Newton's zero-order rainbow caused by refraction only [7], which was expected by Newton [2] but not realized in the meteorological rainbow. Nuclear rainbows have been extensively studied [8–19] and found to be very important in uniquely determining nucleus-nucleus interactions. The determined global deep potentials have been powerful in understanding nuclear cluster structures and nuclear rainbows in a unified way [20–24]. Also, new concepts of prerainbow [7], dynamically refracted primary bow [25], dynamically generated secondary bow [14, 26], ripples superimposed on the Airy structure [15], and quasinuclear rainbows [27] have been developed.

The existence of a secondary bow is not expected in principle in nuclear rainbow scattering caused by refraction due to an attractive nuclear potential. In fact, in the semiclassical theory of nuclear scattering [28–31] within a mean-field nuclear potential, only one extremum (i.e., only one rainbow) is allowed in the deflection function. However, the existence of a secondary bow has been demonstrated in the asymmetric ^{16}O+^{12}C [14] and ^{13}C+^{12}C rainbow scattering [26]. The secondary bow is generated dynamically [14, 26] by a quantum coupling to the excited states in the classically forbidden dark side of the primary

Newton's zero-order rainbow, which is caused by the astigmatism of a Luneburg-lens-like mean-field nuclear potential [7, 32, 33]. However, to the authors' best knowledge, no evidence of a secondary bow has been noticed for the thoroughly studied symmetric ^{12}C+^{12}C system [34–48].

The nuclear rainbow in ^{12}C+^{12}C elastic scattering was first reported in Refs. [34–36]. The experimental angular distribution measured at the incident energy E_L =300 MeV by Bohlen *et al.* [36] was reproduced well up to $\theta_{\rm c.m.}$=63°, except for the rise at the largest angle of 70.4°, in the folding model with a coupling to the 2^+ (4.44 MeV) of ^{12}C. The nuclear rainbow angle $\theta^R_{\rm c.m.}\approx$56° was determined from the deflection function. Bohlen *et al.* [37] also measured the angular distribution at E_L=240 MeV up to $\theta_{\rm c.m.}$=60°. They observed a clear first-order Airy minimum (A1) at $\theta_{\rm c.m.}\approx$40° followed by the fall-off of the cross sections in the dark side of the nuclear rainbow. Demyanova *et al.* [38, 39] extended the measurement of the angular distribution at E_L=240 MeV to a much larger angle of 93°, which showed that the angular distribution does not fall monotonically beyond 60°, similar to the case at 300 MeV.

Thus, the experimental angular distributions in rainbow scattering for ^{12}C+^{12}C at E_L =240-300 MeV [36–39] have not been reproduced at large angles beyond 60° toward 90° in intensive calculations performed on purpose [37–40]. Despite extensive studies of ^{12}C+^{12}C scattering [38–45], the discrepancy between theory and experiment remains unsolved. Obviously, ^{12}C+^{12}C rainbow scattering cannot be understood within the frame of the ordinary theory of nuclear rainbow [28–31]. No attention has been paid to the physical meaning and the origin of the anomalous structure of the angular distributions beyond 60° in the fall-off region.

The purpose of this paper is to report, for the first time, the emergence of a secondary bow with ripples in ^{12}C+^{12}C rainbow scattering at both E_L =240 and 300 MeV. We investigate the angular distribution of ^{12}C+^{12}C rainbow scattering using the coupled channels (CC) method with an extended double folding potential derived from realistic microscopic wave functions for ^{12}C and a density-dependent effective two-body force. This third finding, alongside the ^{16}O+^{12}C and ^{13}C+^{12}C systems, reinforces the concept of secondary bow in nuclear rainbow scattering. The mechanism of the secondary bow is investigated.

2 The extended double folding model

We study rainbow scattering for the ^{12}C+^{12}C system with an extended double folding (EDF) model that describes all the diagonal and off-diagonal coupling potentials derived from the microscopic realistic wave functions for ^{12}C using a density-dependent effective nucleon-nucleon force. The diagonal and coupling potentials for the ^{12}C+^{12}C system are calculated using the EDF model as follows:

$$V_{ij,kl}(\mathbf{R}) = \int \rho^{(^{12}\mathrm{C})}_{ij}(\mathbf{r}_1)\, \rho^{(^{12}\mathrm{C})}_{kl}(\mathbf{r}_2) \times v_{NN}(E,\rho,\mathbf{r}_1+\mathbf{R}-\mathbf{r}_2)\, d\mathbf{r}_1 d\mathbf{r}_2, \quad (1)$$

where $\rho^{(^{12}\mathrm{C})}_{ij}(\mathbf{r})$ represents the diagonal ($i = j$) or transition ($i \neq j$) nucleon density of ^{12}C which is calculated using the microscopic three α cluster model in the resonating group method [49]. This model well reproduces the α cluster and shell-like structures of ^{12}C, and the wave functions have been checked against much experimental data, including charge form factors and electric transition probabilities [49]. In the calculations, we take into account the excitation of the 2^+, 3^- (9.64 MeV) and 4^+ (14.08 MeV) states of ^{12}C. For the effective nucleon-nucleon interaction ($v_{\rm NN}$), we use the DDM3Y-FR interaction [50–52], which accounts for the finite-range nucleon exchange effect [41]. We introduce the normalization factor N_R [48] for the real double folding potential. An imaginary potential with a Woods-Saxon volume-type (nondeformed) form factor is phenomenologically introduced to account for the effect of absorption due to other channels.

3 Emergence of a secondary nuclear rainbow

In Fig. 1, the angular distributions for elastic ^{12}C+^{12}C scattering at E_L= 240 and 300 MeV, calculated using the CC method with the six-channel couplings of (^{12}C(I^π), ^{12}C(J^π)) = (0^+, 0^+), (0^+, 2^+), (0^+, 3^-), (0^+, 4^+), (2^+, 2^+), and (2^+ , 4^+),

are displayed in comparison with the experimental data [36–39]. We used N_R = 1.13 and 1.20 for the real potential at 240 and 300 MeV, respectively. For the imaginary potential the strength parameters W=18 and 19 MeV for E_L=240 and 300 MeV, respectively, were found to fit the data with fixed radius and diffuseness parameters R_W=5.6 fm and a_W=0.7 fm.

The calculated symmetrized angular distributions (solid lines) show good agreement with the experimental data up to 70°. Our calculations accurately reproduce the Airy minima at both 240 MeV and 300 MeV. At 240 MeV, our calculations also reproduce the oscillatory ripple pattern for angles beyond 70°, although the magnitude is somewhat larger than the experimental data. We also successfully reproduce the angular distribution at 300 MeV, including the final data point at 70°, where the cross section appears to begin to rise. It is highly desirable to measure the angular distribution at large angles at 300 MeV to confirm the predicted ripple oscillations. These good fits to the data at 240 MeV and 300 MeV are much better than the latest calculations in Refs. [40, 45].

We note the rise of the cross sections both at 240 and 300 MeV beyond $\theta_{\rm c.m.}\approx 60°$ in the fall-off region of the primary nuclear rainbow and the appearance of a broad bump toward 90° in the calculated unsymmetrized angular distributions shown as dashed blue lines. This resembles the secondary bow observed in the asymmetric ^{13}C+^{12}C scattering, where a bump of the secondary bow appears at $\theta_{\rm c.m.}\approx 70°$ (Fig. 1 of Ref. [26]).

To analyze this, we decomposed the calculated angular distributions into farside and nearside components, following the powerful prescription of Refs. [53, 54]. This method has been very effective in studying the Airy minimum in rainbow scattering, including two bosonic identical nuclei ^{12}C+^{12}C [55, 56] and ^{16}O+^{16}O [9, 57]. The farside component is shown by the pink dotted lines. We find that the enhanced cross sections of the bump in the angular distributions beyond $\theta_{\rm c.m.}\approx 60°$ are due to refractive farside scattering. The first order Airy minimum $A1^{(P)}$ of the primary nuclear rainbow is determined at 43° for E_L=240 MeV and at 33° for 300 MeV, respectively. The Airy minimum of the secondary bow $A1^{(S)}$ is located at $\theta_{\rm c.m.}$=77° for 240 MeV and 63° for 300 MeV, respectively.

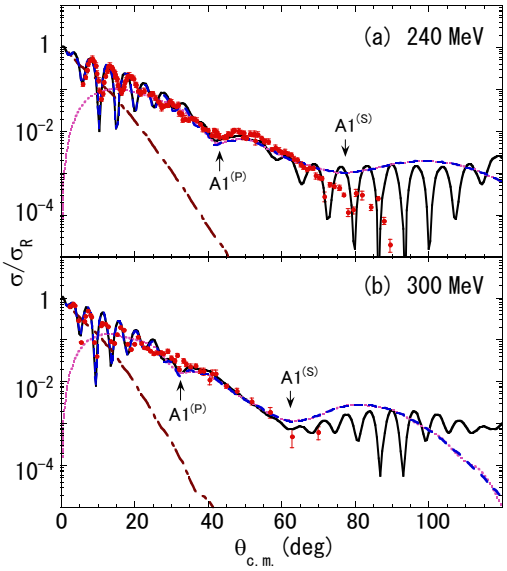


Fig. 1 Angular distributions in ^{12}C+^{12}C scattering at (a) E_L = 240 MeV and (b) 300 MeV, calculated with the six-channel couplings, are displayed (as a ratio to Rutherford scattering) as black solid lines in comparison with the experimental data (points) from Refs. [36–39]. The results without symmetrization of two bosonic identical nuclei are displayed by blue dashed lines. The calculated farside and nearside components are given by pink dotted lines and brown dash-dotted lines, respectively. $A1^{(P)}$ and $A1^{(S)}$ stand for the Airy minimum of the primary nuclear rainbow and the secondary bow, respectively

We note that the experimental angular distribution beyond ∼70° at 240 MeV shows oscillations, and the rise of the last data point of the angular distribution at 300 MeV is an indication of the start of the secondary bow. The present calculations (solid lines) reproduce these characteristic oscillatory features of the angular distributions at large angles toward 90°. The oscillations are due to symmetrization of identical two bosonic nuclei, which causes interference between the scattering amplitudes at $\theta_{\rm c.m.}$ and 180-$\theta_{\rm c.m.}$. The interference breaks up the bright bump of the secondary bow, producing the ripples, which makes it difficult to intuitively notice the existence of the bright secondary bow in symmetric ^{12}C+^{12}C rainbow scattering, unlike in the asymmetric ^{16}O+^{12}C and ^{13}C+^{12}C systems.

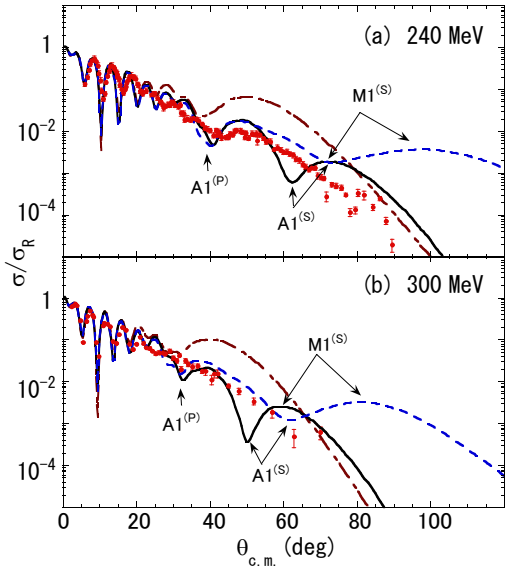


Fig. 2 The angular distributions for ^{12}C+^{12}C scattering calculated without symmetrization at (a) E_L=240 and (b) 300 MeV are displayed (as a ratio to Rutherford scattering) for: single-channel calculations (dash-dotted lines), two-channel calculations (solid lines), and three-channel calculations (dashed lines). These are compared with the experimental data (points) from Refs.[37–39]. $A1^{(P)}$ stands for the Airy minimum of the primary nuclear rainbow, while $A1^{(S)}$ and $M1^{(S)}$ represent the Airy minimum and maximum of the secondary bow, respectively

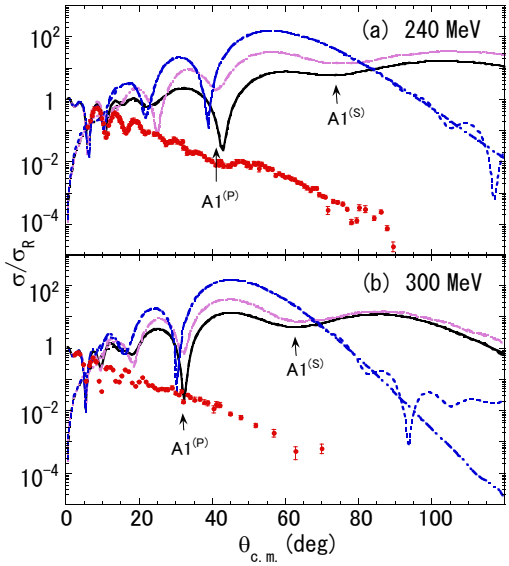


Fig. 3 The unsymmetrized total (farside) angular distributions for ^{12}C+^{12}C scattering at (a) 240 MeV and (b) 300 MeV, calculated with W=0, are displayed (as a ratio to Rutherford scattering) by the blue dash-dot-dot lines (blue dashed lines) for the single-channel coupling, pink dashed lines (pink dotted lines) for the three-channel coupling, and black solid lines (black dot-dash lines) for the six-channel coupling. The farside components are indistinguishable from the total angular distributions in the rainbow region including $A1^{(P)}$ and $A1^{(S)}$. The experimental data (points) are from Refs. [36–39]

4 Origin of a secondary bow and ripples

To investigate which coupling is responsible for the generation of the secondary bow with the Airy minimum $A1^{(S)}$, we display in Fig. 2 the angular distributions calculated under three different coupling scenarios: (1) in the single channel, (2) with two-channel coupling including (0^+, 0^+) and (0^+, 2^+), and (3) with three-channel coupling including (0^+, 0^+), (0^+, 2^+), and (2^+, 2^+) channels. It is clear that the single-channel calculations produce only the first-order Airy minimum $A1^{(P)}$ of the primary nuclear rainbow, and the angular distributions in the dark side fall monotonically at large angles toward 90°. We observe that $A1^{(S)}$ and the bright bump of the Airy maximum $M1^{(S)}$ of the secondary bow, appearing before the fall-off, are already created by the two-channel coupling. By including mutual excitation to the 2^+ state in the three-channel coupling, $A1^{(S)}$ and $M1^{(S)}$ shift to larger angles, becoming closer to the calculations with the six-channel coupling shown in Fig. 1. Thus, coupling to the 2^+ state with reorientation [26] is essential for creating the secondary bow.

Fig. 3 clearly shows the Airy minima $A1^{(P)}$ and $A1^{(S)}$ in calculations performed with a reduced imaginary potential W=0. In the single-channel calculations (blue dash-dot-dot lines), only $A1^{(P)}$ is distinctly observed at 240 and 300 MeV. For the three-channel calculations, the primary rainbow's fall-off is replaced by enhanced cross sections, forming a bright region of the secondary bow with $A1^{(S)}$, while the position of $A1^{(P)}$ is only slightly shifted backward compared to calculations without couplings. The six-channel calculations (solid lines) exhibit $A1^{(P)}$ at 43° and $A1^{(S)}$ at 77° for 240 MeV, and $A1^{(P)}$ at 33° and $A1^{(S)}$ at 63° for 300 MeV. As seen in Fig. 3, the farside components are indistinguishable from the total angular distributions in the regions of $A1^{(P)}$ and $A1^{(S)}$ of the Airy structure. This observation indicates that the secondary bow with $A1^{(S)}$ originates from refractive farside scattering.

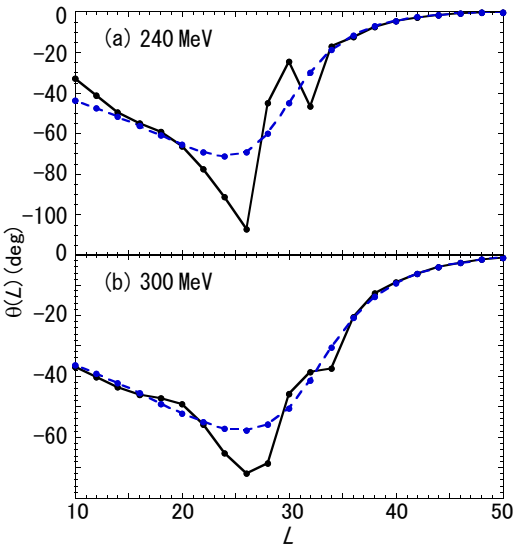


Fig. 4 The deflection functions for ^{12}C+^{12}C scattering, calculated with W=0 in the six-channel coupling (solid lines) and in the single-channel (dashed lines), are displayed at 240 and 300 MeV. The line is to guide the eye

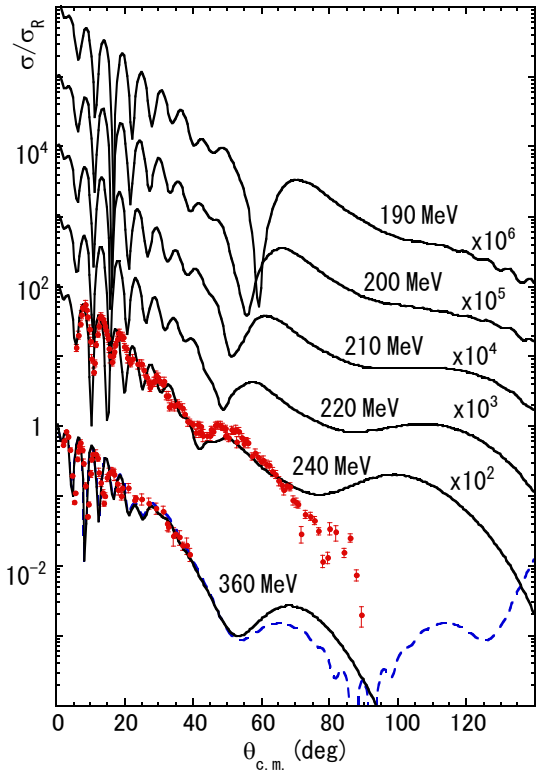


Fig. 5 Angular distributions calculated without symmetrization at energies above 190 MeV with the six-channel coupling are displayed (as a ratio to Rutherford scattering) as solid lines. At 360 MeV, dashed lines represent the symmetrized calculated angular distribution in comparison with the experimental data (points) from Ref. [60]

In Fig. 4, while the single-channel calculations show one extremum in the deflection functions, corresponding to the primary nuclear rainbow angle, the CC calculations show more than one extremum. The secondary bow, which corresponds to the second minimum, is dynamically caused by quantum coupling to the internal structure of the ^{12}C nuclei. While Newton's zero-order primary nuclear rainbow is caused by the radially monotonic mean field potential and involves no internal structure, the secondary bow is created due to the dynamical polarization potential with undulations [17]. The undulations of the deflection function arise from the undulations of the polarization potential, which appears even in the intermediate radial region due to the coupling to the 2^+ state of ^{12}C. This explains why it was not possible to reproduce the angular distributions for ^{12}C+^{12}C rainbow scattering up to large angles toward 90° with the mean field potential alone, without the dynamically generated polarization potential with undulations. In Fig. 4, we note that partial waves (trajectories) with larger L values than those for the primary rainbow are involved. This means that the secondary bow emerges in the outer region of the nucleus where the inelastic scattering to the 2^+ state occurs, and the refractive scattering of the primary rainbow is strongly damped.

Since a secondary bow is not seen in the experimental angular distributions at 139.5 and 158.8 MeV in Refs. [58, 59], we investigate at what energy the secondary bow emerges. In Fig. 5, the angular distributions calculated with the six-channel coupling at E_L=190-360 MeV, using the potential at 240 MeV (except N_R=1.2 for 360 MeV), are displayed. At 200 MeV, the fall-off in the dark side of the primary rainbow, with $A1^{(P)}$ at 56° and $M1^{(P)}$ at 66° in the bright side, continues toward large angles, showing no indication of a secondary bow. At 210 MeV, this fall-off stops, and a plateau appears at around 90°, followed by a new fall-off beyond 120°. At 220 MeV, we observe a clear minimum, $A1^{(S)}$, at 88°, and the bump of the secondary bow, $M1^{(S)}$, at 108°. Thus,

we find that the secondary bow starts to emerge at around 210 MeV and develops as the incident energy increases.

The calculation accurately reproduces the experimental data at 360 MeV from Ref. [60]. The calculation places the $A1^{(P)}$ at around 25° and predicts the secondary bow with $A1^{(S)}$ at around 54° and $M1^{(S)}$ at around 70°. The secondary bow is predicted to persist at least as high as 360 MeV.

At this higher energy, ripples from symmetrization, which characterize the secondary rainbow of the symmetric ^{12}C+^{12}C system and can obscure the original $M1^{(S)}$ bump, appear near 90°. This makes it difficult to recognize the existence of a secondary rainbow in experimental data. However, these ripples will disappear in the secondary rainbow for the ^{12}C+$^{13}_{\Lambda}$C system, because the Λ hyperon breaks bosonic symmetrization. In fact, the $M1^{(S)}$ bump of the secondary rainbow, now without ripples, has been confirmed in experimental data from ^{13}C + ^{12}C scattering, where an extra neutron similarly breaks bosonic symmetrization (see Fig. 1 of Ref. [26]). It is worth mentioning that ripples arise from the symmetrization of two bosonic identical nuclei [61] in refractive scattering, not solely from the symmetrization of either the farside or nearside scattering amplitude.

The reason why the secondary bow is generated above E_L=210 MeV is that the contribution to the elastic scattering cross sections from channel couplings, predominantly from the 2^+ state of ^{12}C, increases relative to the cross sections solely due to the elastic channel. The latter decreases exponentially at large angles in the fall-off region on the dark side of the primary nuclear rainbow. The inelastic scattering to the 2^+ state, which is shown in Fig. 6, is very strong, and its cross sections even exceed those of other inelastic and even elastic channels in the rainbow region. As the incident energy increases, the $A1^{(P)}$ of the primary rainbow shifts to forward angles, which causes the fall-off to shift forward. Thus, the cross sections in the fall-off region of the primary rainbow decrease rapidly as energy increases, which enhances the prominence of the bump of the secondary bow, $M1^{(S)}$. Thus, the secondary bow is generated dynamically at energies above 210 MeV.

Finally, we mention that the long-standing problem concerning the Airy minima and Airy elephants in ^{12}C+^{12}C scattering has been resolved after decades of concern by recognizing the existence of a dynamically generated secondary rainbow [62].

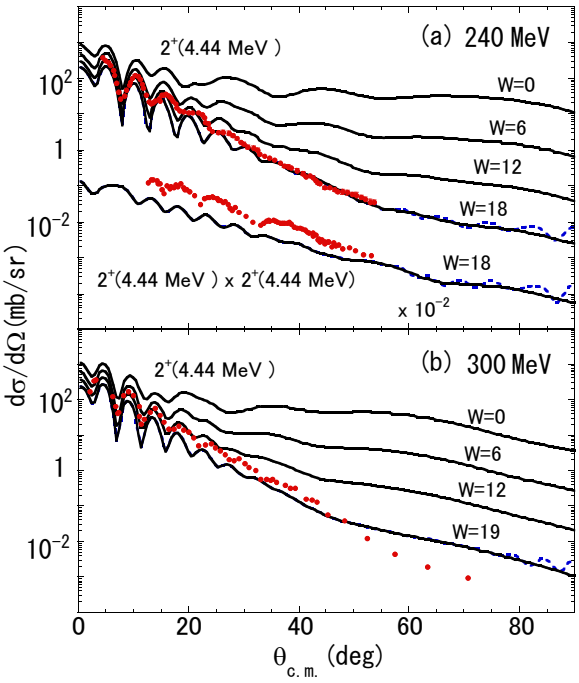


Fig. 6 Angular distributions for inelastic ^{12}C+^{12}C scattering with excitation to the 2^+ state at (a) E_L=240 and (b) 300 MeV, calculated with the six-channel coupling (solid lines), are displayed in comparison with the experimental data (points) from Refs. [36–39]

5 Summary

We have, for the first time, shown the emergence of a secondary bow with ripples in the angular distributions of symmetric ^{12}C+^{12}C rainbow scattering at E_L=240 and 300 MeV. To achieve this, we utilized an extended double-folding model with coupled-channel calculations, incorporating diagonal and off-diagonal potentials derived from microscopic wave functions of ^{12}C. This finding, alongside the asymmetric systems ^{16}O+^{12}C and ^{13}C+^{12}C, reinforces the concept of a secondary bow in nuclear rainbow scattering. We suggest that a secondary bow exists widely in nuclear rainbow scattering involving ^{12}C, such as ^{12}C+^{13}N, ^{12}C+^{14}C, ^{12}C+^{15}C, ^{12}C+$^{13}_{\Lambda}$C, and ^{12}C+$^{17}_{\Lambda}$O.

- Funding No funding.

- Conflict of interest/Competing interests Not applicable
- Consent for publication The authors agree with publication of the manuscript in the traditional publishing model.
- Data availability Statement This manuscript has no associated data or the data will not be deposited. [Authors' comment: This is a theoretical study using published data, and all data information is properly referenced.]
- Code availability Code/Software sharing not applicable to this article as this manuscript has no associated code/software.

References

[1] R. Descartes, *Le Discours de la Methode (sous-titre: Pour bien conduire sa raison, et chercher la verité dans les sciences) plus la Dioptrique, Les Meteores et la Geometrie* (Leiden, 1637; Hackett Publishing, Cambridge, 2001)

[2] I. Newton, *Opticks or, a Treatise of the Reflexions, Refractions, Inflexions Colours of Light* (London, 1704; Dover Publications, New York, 1952)

[3] G. B. Airy, Trans. Camb. Philos. Soc. **6**, 379 (1838)

[4] H. M. Nussenzveig, Sci. Am. **236**, 116 (1977)

[5] J. A. Adam, Phys. Rep. **356**, 229 (2002)

[6] D. A. Goldberg, S. M. Smith, G. F. Burdzik, Phys. Rev. C **10**, 1362 (1974)

[7] F. Michel, G. Reidemeister, S. Ohkubo, Phys. Rev. Lett. **89**, 152701 (2002)

[8] D. T. Khoa, W. von Oertzen, H. G. Bohlen, S. Ohkubo, J. Phys. G **34**, R111 (2007)

[9] F. Michel, G. Reidemeister, S. Ohkubo, Phys. Rev. C **63**, 034620 (2001)

[10] A. A. Ogloblin *et al.*, Phys. At. Nucl. **66**, 1478 (2003)

[11] S. Ohkubo Y. Hirabayashi, Phys. Rev. C **70**, 041602(R) (2004)

[12] S. Ohkubo Y. Hirabayashi, Phys. Rev. C **75**, 044609 (2007)

[13] Sh. Hamada, Y. Hirabayashi, N. Burtebayev, S. Ohkubo, Phys. Rev. C **87**, 024311 (2013)

[14] S. Ohkubo Y. Hirabayashi, Phys. Rev. C **89**, 051601(R) (2014)

[15] S. Ohkubo Y. Hirabayashi, Phys. Rev. C **89**, 061601(R) (2014)

[16] S. Ohkubo, Y. Hirabayashi, A. A. Ogloblin, Yu. A. Gloukhov, A. S. Dem'yanova, W. H. Trzaska, Phys. Rev. C **90**, 064617 (2014)

[17] R. S. Mackintosh, Y. Hirabayashi, S. Ohkubo, Phys. Rev. C **91**, 024616 (2015)

[18] S. Ohkubo Y. Hirabayashi, Phys. Rev. C **92**, 024624 (2015)

[19] Yu. A. Glukhov, V. P. Rudakov, K. P. Artemov, A. S. Demyanova, A. A. Ogloblin, S. A. Goncharov, A. Izadpanakh, Phys. At. Nucl. **70**, 1 (2007)

[20] F. Michel, S. Ohkubo, G. Reidemeister, Prog. Theor. Phys. Suppl. **132**, 7 (1998)

[21] S. Ohkubo, T. Yamaya, P. E. Hodgson, Nuclear clusters, in *Nucleon-Hadron Many-Body Systems*, edited by H. Ejiri H. Toki (Oxford University Press, Oxford, UK, 1999), p. 150

[22] S. Ohkubo K. Yamashita, Phys. Lett. B **578**, 304 (2004)

[23] S. Ohkubo Y. Hirabayashi, Phys. Lett. B **684**, 127 (2010)

[24] Y. Hirabayashi S. Ohkubo, Phys. Rev. C **88**, 014314 (2013)

[25] S. Ohkubo Y. Hirabayashi, Phys. Rev. C **94**, 034601 (2016)

[26] S. Ohkubo, Y. Hirabayashi, A. A. Ogloblin, Phys. Rev. C **92**, 051601(R) (2015)

[27] S. Ohkubo, Phys. Rev. C **109**, 034618 (2024)

[28] K. W. Ford J. A. Wheeler, Ann. Phys. (N. Y.) **7**, 259 (1959)

[29] R. G. Newton, *Scattering Theory of Waves Particles* (McGraw-Hill Book Company, New York, 1966)

[30] P. E. Hodgson, *Nuclear Heavy-Ion Reactions* (Oxford Studies in Nuclear Physics, Clarendon Press: Oxford University Press, Oxford, UK, 1978)

[31] D. M. Brink, *Semi-classical Methods for Nucleus-Nucleus Scattering* (Cambridge University Press, Cambridge, 1985)

[32] R. K. Luneburg, *Mathematical Theory of Optics* (University of California Press, Cambridge, 1965)

[33] S. Ohkubo, Phys. Rev. C **93**, 041303(R) (2016)

[34] M. Buenerd, P. Martin, R. Bertholet, C. Guet, M. Maurel, J. Mougey, H. Nifenecker, J. Pinston, P. Perrin, F. Schussler, J. Julien, J. P. Bondorf, L. Carlen, H. A. Gustafsson, B. Jakobsson, T. Johansson, P. Kristiansson, O. B. Nielsen, A. Oskarsson, I. Otterlund, H. Ryde, B. Schroder, Q. Tibell, Phys. Rev. C **26**, 1299 (1982)

[35] M. E. Brandan, Phys. Rev. Lett. **49**, 1132 (1982)

[36] H. G. Bohlen, M. R. Clover, G. Ingold, H. Lettau, W. von Oertzen, Z. Phys. A **308**, 121 (1982)

[37] H. G. Bohlen, X. S. Chen, J. G. Cramer, P. Fröbrich, B. Gebauer, H. Lettau, A. Miczaika, W. von Oertzen, R. Ulrich, T. Wilpert, Z. Phys. A **322**, 241 (1985)

[38] A.S. Demyanova, S.A. Goncharov, HG. Bohlen, A.N. Danilov, S.V. Khlebnikov, V.A. Maslov, A.A. Ogloblin, Yu.E. Penionzkevich, Yu.G. Sobolev, W. Trzaska, G.P. Tyurin, AIP Conference Proceedings on *International Symposium on Exotic Nuclei*, edited by Yu. E. Penionzhkevich S. M. Lukyanov, **1224**, 82 (2010)

[39] A.S. Demyanova, H.G. Bohlen, A.N. Danilov, S.A. Goncharov, S.V. Khlebnikov, V.A. Maslov, Yu.E. Penionzkevich, Yu.G. Sobolev, W. Trzaska, G.P. Tyurin, A.A. Ogloblin, Nucl. Phys. A **834**, 473c (2010)

[40] D.T. Khoa, N.H. Phuc, D.T. Loan, B.M. Loc, Phys. Rev. C **94**, 034612 (2016)

[41] D.T. Khoa, W. von Oertzen, H.G. Bohlen, Phys. Rev. C **49**, 1652 (1994)

[42] A. Hemmdan, Fatma O. M. Al Mahmody, M.A. Hassanain, J. Phys. Soc. Japan **90**, 094201 (2021)

[43] T. Furumoto, W. Horiuchi, M. Takashina, Y. Yamamoto, Y. Sakuragi, Phys. Rev. C **85**, 044607 (2012)

[44] M.A. Hassanain, A.A. Ibraheem, M.El-Azab Farid, Phys. Rev. C **77**, 034601 (2008)

[45] N.H. Phuc, D.T. Khoa, N.T.T. Phuc, and D.C. Cuong, Eur. Phys. J. A **57**, 75 (2021)

[46] M.E. Brandan, S.H. Fricke, K.W. McVoy, Phys. Rev. C **38**, 673 (1988)

[47] M.E. Brandan, M. Rodríguez-Villafuerte, A. Ayala, Phys. Rev. C **41**, 1520 (1990)

[48] M.E. Brandan G.R. Satchler, Phys. Rep. **285**, 143 (1997)

[49] M. Kamimura, Nucl. Phys. A **351**, 456 (1981)

[50] A.M. Kobos, B.A. Brown, P.E. Hodgson, G.R. Satchler, A. Budzanowski, Nucl. Phys. A **384**, 65 (1982)

[51] A.M. Kobos, B.A. Brown, R. Lindsay, G.R. Satchler, Nucl. Phys. A **425**, 205 (1984)

[52] G. Bertsch, J. Borysowicz, H. McManus, W.G. Love, Nucl. Phys. A **284**, 399 (1977)

[53] R.C. Fuller, Phys. Rev. C **12**, 1561 (1975)

[54] K.W. McVoy G.R. Satchler, Nucl. Phys. A **417**, 157 (1984)

[55] K.W. McVoy, M.E. Brandan, Nucl. Phys. A **542**, 295 (1992)

[56] F. Michel, S. Ohkubo, Eur. Phys. J. A **19**, 333 (2004)

[57] M.P. Nicoli, F. Haas, R.M. Freeman, N. Aissaoui, C. Beck, A. Elanique, and R. Nouicer, A. Morsad, S. Szilner, Z. Basrak, M.E. Brandan, G.R. Satchler, Phys. Rev. C **6**0, 064608 (1999)

[58] S. Kubono, K. Morita, M. H. Tanaka, M. Sugitani, H. Utsunomiya, H. Yonehara, M.-K. Tanaka, S. Shimoura, E. Takada, M. Fukada, K. Takimoto, Phys. Lett. B **127**, 19 (1983)

[59] S. Kubono, M. H. Tanaka, M. Sugitani, K. Morita, H. Utsunomiya, M.-K. Tanaka, S. Shimoura, E. Takada, M. Fukada, K. Takimoto, Phys. Rev. C **31**, 2082 (1985)

[60] M. Buenerd, A. Lounis, J. Chauvin, D. Lebrun, Ph. Martin, G. Duhamel, J.C. Gondrand, P. De Saintignon, Nucl. Phys. A **424**, 313 (1984)

[61] G. R. Satchler, *Direct Nuclear Reactions* (Clarendon Press, New York 1983), p.68

[62] S. Ohkubo, Y. Hirabayashi, Eur. Phys. J. A **61**, 175 (2025)